

Title	Wave farm planning through high-resolution resource and performance characterization
Authors	Carbello, R.;Arean, N.;Alvarez, M.;Lopez, I.;Castro, A.;Lopez, M.;Iglesias, Gregorio
Publication date	2018-12-23
Original Citation	Carballo, R., Arean, N., Álvarez, M., López, I., Castro, A., López, M. and Iglesias, G. (2019) 'Wave farm planning through high-resolution resource and performance characterization', Renewable Energy, 135, pp. 1097-1107. doi: 10.1016/j.renene.2018.12.081
Type of publication	Article (peer-reviewed)
Link to publisher's version	http://www.sciencedirect.com/science/article/pii/S0960148118315283 - 10.1016/j.renene.2018.12.081
Rights	© 2018 Published by Elsevier Ltd. This manuscript version is made available under the CC-BY-NC-ND 4.0 license - http://creativecommons.org/licenses/by-nc-nd/4.0/
Download date	2023-05-07 19:25:18
Item downloaded from	http://hdl.handle.net/10468/7353

Wave farm planning through high-resolution resource and performance characterization

R. Carballo^{1*}, N. Areal¹, M. Álvarez¹, I. López¹, A. Castro², M. López³, G. Iglesias^{4,5}

¹Univ. de Santiago de Compostela, Área de Ingeniería Hidráulica, EPSE Campus Univ. s/n, 27002 Lugo, Spain

²Univ. de Santiago de Compostela, Área de Ingeniería e Infraestructura de los Transportes, EPSE, Campus Univ. s/n, 27002 Lugo, Spain

³Dpto. de Construcción e Ing. de Fabricación, Univ. de Oviedo, EPM, Gonzalo Gutierrez Quiros s/n, 33600, Mieres, Spain

⁴MaREI, Environmental Research Institute & School of Engineering, University College Cork, Ireland

⁵School of Engineering, University of Plymouth, UK

Abstract

Wave farm planning in a coastal region should lead to the selection of: i) the type of technology of wave energy converter (WEC) providing the highest performance at specific sites and ii) the sites for wave farm operation allowing an integrated coastal zone management (ICZM). On these bases, the deployment of a wave farm should be based on an accurate analysis of the performance of different WECs at coastal locations where wave energy exploitation does not interfere with other coastal uses, and the environmental impact is minimized (or positive, e.g. allowing coastal protection). With this in view, in this piece of research the intra-annual performance of various WECs of the same type (buoy-type) is computed at different locations in NW Spain allowing an ICZM perspective. For this purpose, the intra-annual version of WEDGE-p[®] (Wave Energy Diagram Generator – performance) tool is implemented. The results show that, as opposed to previous analysis on WECs with different principle of operation, the level of performance of buoy-type WECs at specific locations may present strong similarities. In this case, an accurate computation of different performance parameters along with their joint analysis emerge as a prerequisite for an informed decision-making.

Keywords: Wave energy; Buoy-type WECs; ICZM; Intra-annual performance

*Corresponding author. Tel.: +34-982-285900; fax.: +34-982-285926.

E-mail address: rodrigo.carballo@usc.es

1. Introduction

Wave energy exploitation represents a major technological challenge due to the need of wave energy converters (WECs) to operate under harsh conditions [1]. Nevertheless, the intense research developed over the last years has led to an increase in WECs' efficiency and a better response under extreme conditions. As a result, a large number of different WECs are currently available, which may be classified based on three aspects: i) distance to the coast, ii) shape and direction and iii) mode of operation [2]. The latter is usually considered the most relevant aspect, according to which three main technologies are usually defined: overtopping devices (OTDs) [3,4], oscillating water columns [5-7] (OWCs), and wave activated bodies (WABs) [8,9].

The most appropriate device for a specific coastal site is function of several aspects. In this context, the magnitude of the resource and its spatial and temporal distribution is of paramount importance. This is caused by their efficiency, which depends on the wave resource characteristics, namely wave height and period. Thus, the device providing the highest performance is site-specific and no general recommendation can be drawn. On these bases, the selection of the most efficient WEC-site combination should be conducted based on a thorough analysis of the performance of several combinations; to this end, it has been shown that an exhaustive study on the wave resource distribution following specific procedures is required [10]. In this regard, the wave energy resource may experience significant modifications in short distances caused by the different coastal processes resulting from the interaction of waves with the seabed in their propagation to the coast [11]. In addition, the coastal regions of interest for wave energy exploitation usually exhibit a considerable temporal variability in the resource, with

abrupt seasonal or even monthly variations [12,13], which need to be considered for an appropriate performance analysis [14].

Last but not least, wave energy exploitation represents a new coastal use which has to be considered under an integrated coastal zone management (ICZM) approach [15,16] so as to avoid the interference with other coastal uses along with environmental damage, thereby leading to a sustainable development of the coast [17-19]. With this aim, an ICZM perspective has to be considered for conducting the final decision-making when deploying a wave farm in a coastal area (i.e. definition of the most appropriate WEC-site combination).

In this piece of research, the intra-annual performance of three WABs of buoy type: Aquabuoy, Bref-HB and F-2HB [20-23], is thoroughly investigated. This specific technology is selected insofar as several wave farms of this type have been proposed over the last years in the Galician region e.g. [24]; however, limited studies on the performance of these devices under real conditions have been conducted. The main characteristics of the selected WECs are shown in Table 1. The performance of these devices is analyzed at different sites within the Galicia coast (NW Spain) (Figure 1) compatible with an ICZM approach.

This study is conducted by implementing the intra-annual version of the recently patented tool WEDGE-p[®] (Wave Energy Diagram Generator - performance) [25]. The tool is now available within a brand-new interface allowing the self-contained computation of the relevant intra-annual performance parameters of WECs at the locations of interest, which in turn are selected through a Geographical Information System (GIS) viewer, containing the relevant socioeconomic and environmental spatial data in the region.

[FIGURE 1]

[TABLE 1]

The paper is structured in five sections. In first place, in Section 2, the data requirements both in terms of wave characterization and from an environmental and socioeconomic standpoint are presented. Then, in Section 3, the procedure followed for implementing the tool in the coastal area of interest is briefly discussed. In Section 4, the performance results are thoroughly presented for the different WEC-site combinations of interest. In Section 5, a comprehensive discussion on the implications of the results presented is conducted. Finally, the main conclusions are established in Section 6.

2. Data requirements for wave energy exploitation decision-making

The wave data currently available in most of the coastal areas are not sufficient for an appropriate decision-making when deploying a wave farm. This limitation results, in first instance, from how WECs operate. The efficiency is usually given through a power matrix which provides the power output, P , for the different wave conditions usually expressed in terms of significant wave height, H_{m0} , and wave energy period, T_e . In Figure 2 the power matrices of the devices selected are presented. It can be observed that the power output strongly varies depending on the existing conditions, presenting the highest efficiency within an approximately narrow band of H_{m0} in the range of 4-7 m, and a wider range of T_e , roughly 6-13 s. These characteristics of the resource will

cause a significant variation in the performance attained by the selected WECs at different locations; nevertheless, this variation is not likely to be as abrupt as when comparing devices with different principle of operation, which usually attain the highest efficiency in bands of H_{mo} and T_e greatly differing amongst them.

[FIGURE 2]

Furthermore, the way in which the efficiency is provided by device developers causes that the wave energy resource should be characterized following specific procedures allowing the computation of the so-called characterization matrices containing the occurrence and total energy provided by the different wave conditions [10]. Therefore, by combining the WEC's power matrix with the characterization matrix at a site of interest with the same level of resolution, the power performance of a specific WEC-site combination is obtained. In this context, the intra-annual figures of the performance need to be analyzed for which the characterization matrices obtained should correspond with the temporal period capable of reflecting the intra-annual variability of the resource.

Finally, when selecting the sites for wave energy exploitation at which the aforementioned characterization matrices are computed, as stated, the socioeconomic and environmental aspects should be considered so as to avoid the interference with other coastal uses and environmental damage, thereby leading to an effective ICZM.

With this in view, the intra-annual version of the brand new tool WEDGE-p[®] [25], based on complex wave resource characterization methodologies [10] considering high-

resolution numerical modelling, instrumental wave data, along with a vast amount of environmental and socioeconomic information, is implemented and used to evaluate the performance of the selected WECs. The tool provides the resource information in the form of monthly characterization matrices with any desired resolution of wave intervals at the coastal sites of interest, from which it automatically computes the performance of any WEC in terms of various parameters (Section 3). In addition, it also incorporates a Geographical Information System (GIS) viewer including the existing coastal uses and environmental data, e.g.: transport routes, fishing and shellfish areas, environmental protected zones, etc. Therefore, by combining the socioeconomic and environmental information with the resource and performance data obtained, an informed decision-making can be conducted. In the next section, the principal characteristics of the tool and its implementation to the coastal area of interest are presented.

3. Tool development and implementation

3.1. Intra-annual WEDGE-p[®] development

The procedure followed for developing the present tool is based on the deepwater energy bin concept [26] and its numerical propagation towards the coast. On these bases, the most representative offshore energy bins, i.e., trivariate combinations or intervals of significant wave height, H_{m0} , energy period, T_e and wave direction, θ_m , with a specific resolution, are selected and propagated towards the coastal area of interest. The energy bins considered are obtained from the nearest offshore buoy, representative of the surrounding deepwater area, by analyzing a 122712 hourly sea states recorded over a total of 15 years. The resolution of energy bins is established at 0.5 m of H_{m0} , 0.5

s of T_e and 22.5 of θ_m . Then, the most energetic bins providing 95% of the total energy available are retained, representing almost 100% of the exploitable resource [27].

Next, the offshore energy bins retained are propagated towards the coast through high-resolution spectral numerical modelling. More specifically, the SWAN (Simulating WAves Nearshore) model is implemented, being commonly used in wave resource assessments [28-32]. In particular, the model has been previously implemented to this coastal region and successfully validated against field data [27,33]. The model is capable of accurately computing the different wave transformation processes by solving the action balance equation given by:

$$\frac{\partial}{\partial t} N + \nabla \cdot (\vec{C}N) + \frac{\partial}{\partial \theta} (C_\theta N) + \frac{\partial}{\partial \sigma} (C_\sigma N) = \frac{S_t}{\sigma} \quad (1)$$

where N stands for the wave action density, t is the time, C represents the propagation velocity in the geographical space, θ and σ are the direction of the waves and the relative frequency, respectively, C_θ and C_σ represent the propagation velocities in the θ - and σ - space, respectively, and finally, S is the source term given by:

$$S_t = S_{in} + S_{nl3} + S_{nl4} + S_{wc} + S_f + S_{br} \quad (2)$$

where S_{in} represents the generation by wind, S_{nl3} y S_{nl4} stand for triad and quadruplet wave-wave interactions, respectively, and finally S_{wc} , S_f , S_{br} account for dissipation due to whitecapping, bottom friction and wave breaking, respectively [34]. The area covered by the numerical model grid and its bathymetric configuration is presented in Figure 3. As a result of the numerical propagations a reduced number of energy bins are obtained at each node of the numerical grid, i.e., at each location with a given spatial resolution. In other words, at each coastal site a number of wave conditions with a given

occurrence are made available. In the present case, the occurrence is computed in terms of monthly figures, and thus this information can be used to reconstruct high-resolution monthly characterization matrices at the sites of interest.

[FIGURE 3]

Finally, by combining the resource information contained in the characterization matrices with the efficiency provided by the power matrix of a given WEC, the performance of a specific WEC-site combination is obtained. This is automatically computed by the tool as follows. First, the total energy production of a WEC-site combination, E_0 , is obtained by combining each WEC's power output as provided by the power matrix, P_i , with its corresponding occurrence, $O_{b,i}$, in the characterization matrix of the site, i.e.:

$$E_0 = \sum_{i=1}^n P_i O_{b,i} \quad (3)$$

where n is the total number of energy bins considered. Given that the energy production may greatly differ amongst devices stemming from their different rated power, P_r (Table 1), the computation of further parameters is required to an accurate analysis of the WECs' behavior. In this way, the capacity factor, C_f , is also computed by the tool as:

$$C_f = \frac{E_0}{P_r h} \times 100 \quad (4)$$

Finally, in order to have the full picture of the hydrodynamic performance of the WEC-site combinations selected, the capture width, CW , and capture width ratio, CWR , [20] are also computed. CW is given by:

$$CW = \frac{P}{J} \quad (5)$$

where P (W) is the output power and J the total available power. CWR is obtained as:

$$CWR = \frac{P}{JB} \times 100 \quad (6)$$

where B is the characteristic dimension of the WEC [21,22]. The relevant information for its computation along with the resulting values are presented in Table 2. The aforementioned parameters are automatically determined by WEDGE-p[®] tool, for which the WECs' power matrices currently provided by device developers are incorporated within it. For a more detailed description of the procedure on which this tool is based, the reader is referred to previous research into its development [25,35].

[TABLE 2]

3.2. Application to a case study

WEDGE-p tool is applied to a specific area within the Death Coast of Galicia (NW Spain), the region with largest potential in the Iberian Peninsula, where a WEC of buoy-type has been recently deployed [24] . For this purpose, first, the socioeconomic and environmental information together with the bathymetric data contained in the tool are used for selecting three Points: A, B and C with depths 40.2, 72.0 and 99.4 m,

respectively (Figure 1). These locations are selected so as to it make possible an ICZM approach within which, on one hand wave energy operation does not interfere with other coastal uses, and on the other hand potential environmental impacts are minimised. In this regard, aspects such as the potential impacts of the operation of a wave farm over the adjacent area —either negative or positive, e.g., its capability for coastal protection [36]— are out of the scope of this work. However, they may be of major interest for an ICZM approach and should be analyzed for each case study following specific procedures [37-39] prior to installing a wave farm.

Once defined the locations, their characterization matrices are obtained, both in terms of annual (Figure 4) and intra-annual figures (Figures 5). It can be seen that, despite their being separated by short distances, their resource characteristics present certain differences, as it is apparent by the distribution of energy amongst bins, overall presenting a slight reduction in the total energy available with the reduction of depth. The major part of the energy available is neither provided by extreme sea states nor conditions with low wave height, which in turn are those not retained within 95% of energy level analyzed, and therefore allowing the consideration of virtually 100% of the exploitable resource. Regarding the intra-annual variability in the resource, profound variations in both the distribution of the energy amongst bins and the total energy available are apparent, thereby highlighting the importance of determining the performance during short periods, e.g., in terms of monthly figures. In the next section, the results of the monthly performance for all the WEC-site combinations selected are presented.

[FIGURE 4]

[FIGURE 5]

4. Monthly performance analysis of WEC-site combinations

The monthly performance attained by the selected buoy-type WECs (Aquabuoy, Bref-HB and F-2HB) is computed at the three locations defined for wave energy exploitation allowing an ICZM approach (Section 3.2).

In Figures 6, 7 and 8 the intra-annual energy output E_o and capacity factor C_f expressed in terms of monthly figures are plotted at Points A, B and C respectively for the three technologies. Overall, it can be observed that the magnitude of these parameters presents a strong intra-annual variability, along with significant differences amongst the combinations analyzed.

[FIGURE 6]

[FIGURE 7]

[FIGURE 8]

At the three locations selected, the greatest E_o is provided by F-2HB, followed by Aquabuoy and Bref-HB. In the same way, the greatest E_o is attained by the three technologies at Point C (Figure 8) with mean annual figures of 105.32, 33.54 and 2.23 MWh for F-2HB, Aquabuoy and Bref-HB, respectively, overall showing large differences amongst them in production, of the order of 200% (F-2HB and Aquabuoy) and 5000% (F-2HB and Bref-HB). In addition, they show a similar intra-annual trend,

maintaining the aforementioned positions throughout the year. This pattern can be roughly described by a certain stability in the energy production from January to March with figures clearly higher than the monthly average; then, in April, E_o begins to experience a significant reduction which is maintained until July and August during which the lowest values are obtained. Then, E_o shows a significant increase during September and October levelling out over the last one quarter of the year. In all the combinations the months with the greatest production are January and February, approx. 350-400% higher than that obtained during the months with lowest production, attained in August and closely followed by July.

The same general description in the intraannual variability of E_o applies to the capacity factor, C_f , as established by Equations 3 and 4; nevertheless, the level of performance of the devices analyzed greatly differs from those drawn for E_o . In this case, the device overall providing the highest performance (annual mean), at the three locations selected is Bref-HB, followed by Aquabuoy and F-2HB, i.e., the reverse order of that obtained for E_o ; however, in contrast to E_o results, their positions are not conserved throughout the year, as it is apparent in the case of Aquabuoy technology attaining the highest performance over the first and last one third of the year. In addition, the differences amongst technologies are now more reduced. At point C, again the site allowing the highest performance, the C_f obtained are 20.39, 18.42 and 14.47%, respectively, with differences amongst devices of roughly 10% (Bref-HB and Aquabuoy) and 20% (Bref-HB and F-2HB). This is due to the large disparity in their rated power, which causes that the energy production parameter cannot be solely used to analyze the performance of WECs; in contrast, other parameters such as the equivalent hours, usually considered in wind energy or the capacity factor, as it is the present case, should be computed.

However, in order to have the full picture of the performance of the WEC-sites selected, the parameters capture width, CW , and capture width ratio, CWR , are also computed. In Figures 9, 10 and 11, their results are plotted at Points A, B and C, respectively.

[FIGURE 9]

[FIGURE 10]

[FIGURE 11]

In the case of CW , the largest mean annual figures are provided, in the same way as in the energy output parameter, by F-2HB followed by Aquabuoy and Bref-HB.

Nevertheless, in this case Point C is not that allowing the highest performance for the three technologies; now the greatest values are obtained by F-2HB at location B with a mean annual value of 5.15 m, by Aquabuoy at location B with 1.65 m, and by Bref-HB at location C with 0.13 m, yet similar values are attained at the remaining locations. On the other hand, the marked intra-annual variability previously observed is now much more reduced yet intra-annual variations of up to approx. 200% are still present in the case of Bref-HB. In addition, the intra-annual pattern completely differs from that previously presented; now April and September are the months providing the highest performance in the case of Aquabuoy and F-2HB (although in the latter case, the intra-annual variations are very low), and the summer period in the case of Bref-HB.

Despite of the interest of CW parameter, an accurate comparison between the available and output power requires the consideration of the characteristic dimension of the WEC which leads to the definition of capture width ratio, CWR . The greatest figures of CWR

provided by Aquabuoy with 27.44% at Point B, closely followed by F-2HB with 25.77 % at Point C and at a great distance by Bref-HB with 4.20% at Point C, with again very similar figures amongst locations. Finally, as it could be expected from Eqs. 5 and 6, the spatial (locations A, B and C) and temporal variations (monthly variations) follows the same pattern as that depicted in the case of CW parameter.

5. Discussion

At the three locations selected, the greatest E_o in terms of mean annual figures is provided by F-2HB, followed by Aquabuoy and Bref-HB, being attained by the three technologies at Point C, and showing markedly differences in their production of about 200-5000%, which is expected to be primarily caused by their rated power and not by their efficiency. However, the different energy distribution amongst bins at the three sites of interest is not reflected in significant differences in the resulting performance. In addition, the selected WECs show a similar intra-annual trend, maintaining the aforementioned positions throughout the year with an intra-annual variation in E_o of about 350-400%.

The large disparity in the rated power causes E_o not to be a reliable parameter of energy performance analysis, being utterly necessary to compute other parameters such as the capacity factor, C_f . The results obtained show that this parameter, as it could expected, presents a similar trend in terms of intra-annual variability; however, and in contrast to E_o , the performance attained by the selected WECs is relatively similar, being Bref-HB the device with overall the highest performance (which corresponds to the device with

lowest E_0), followed by Aquabuoy and F-2HB with differences of about 10-20%, and not maintaining their positions throughout the year.

The previous parameters depict the most important aspects of the performance of the WEC-site combinations selected. Nevertheless, they do not accurately reflect their hydrodynamic performance. With this in view, the capture width, CW , and capture width ratio, CWR , are also computed. In the case of CW , the highest performance is attained, as in the case of the energy output, by F-2HB, followed by Aquabuoy and Bref-HB. In addition, as in the case of the previous parameters, the different distribution of the resource amongst energy bins does not result in significant variations in the performance at the different locations of interest. Regarding the intra-annual variability pattern, it differs from that provided by the previous parameters; now, only strong intra-annual variations are apparent in the case of Bref-HB, which in addition presents the greatest values during summer months, in contrast with the results previously presented. This results from the variation in the output power being compensated by the reduction in the total available power, indicating that these WECs maintain an appropriate level of performance over a wide range of conditions. Finally, from the analysis of CWR results, further information emerges. Now, Aquabuoy presents the greatest values, closely followed by F2HB, while the performance of Bref-HB plummets. The low performance attained by Bref-HB—which provides the highest capacity factor—is due to its low surface (perpendicular to wave direction) available for harnessing wave energy in comparison with the other two technologies. These results clearly indicate that despite of the great interest of CW and CWR parameters, the latter being considered as that reflecting more accurately the hydrodynamic performance of WECs, other parameters such as the capacity factor are required for an appropriate analysis of WECs’

performance, in particular for describing the intra-annual variability in the energy production, and for considering other geometric characteristics (in addition to the characteristic diameter) which can be of interest.

On the other hand, it is important to highlight that the results obtained differ to some extent from previous analysis on the performance of WECs at different locations within the same coastal region e.g., [14]. When comparing devices with different principle of operation, the variation in the performance amongst them is usually shown to be larger than in the present case. This is due to the fact that each technology is more adapted to operate in a specific range of wave conditions and therefore the performance is much more sensitive to the resource characteristics at the location selected. In fact, in this case, it can occur that a specific technology provides the highest performance at a given location, while at a close location the greatest figures are attained by other technology [14]. This is not the case of the present study, which is probably the result—in addition to the similarities in the resource characteristics at the locations selected— of analysing WECs with the same principle of operation (buoy-type technologies).

6. Conclusions

In this paper, the intra-annual performance of various buoy-type WECs is computed and analyzed at different coastal locations based on an ICZM approach. For this purpose, the intra-annual version of WEDGE-p[®] tool is implemented to this region, which is developed by using complex procedures considering numerical modelling and an extensive set of instrumental data. As a result, the tool made available contains a large set of new data allowing the self-contained computation of high-resolution

characterization matrices and on their bases different performance parameter of any WEC of interest. In addition, the tool incorporates a GIS viewer with the different coastal uses within the region of interest, along with the areas of environmental interest, which should be combined with the aforementioned wave data so as to lead to a sustainable development of the coast when introducing a new use, as it is the case of wave energy exploitation.

The tool is used to select three locations from an integrated coastal management perspective, i.e., where wave farm operation does not interfere with other coastal uses and the environmental impact is expected to be minimum. Then, the characterization of the resource is obtained, and on their bases the intra-annual performance of three WECs with the same type of technology (buoy-type WAB), Aquabuoy, Bref-HB and F-2HB, is determined in terms of energy output, capacity factor, capture width and capture width ratio.

The results show that the performance largely differs depending on the parameter analyzed. Amongst all of them, the capacity factor and capture width ratio emerge as the most important parameters, capable of both capturing the intra-annual variability in the performance along with reliable figures of the hydrodynamic performance. The disparity in the results obtained highlight the need for considering both parameters so as to appropriately describe the performance of WECs at specific locations, along with accurately reflecting the intra-annual variability in the production and avoiding misleading results arising from considerations regarding the geometric configuration or the rated power.

On the other hand, the results presented in this research differ from those provided by previous works dealing with the performance of WECs with different principle of

operation, in which the differences in their performance have shown to be larger than in the present study. This is due, to a certain extent, to the fact that each type technology is likely to be more adapted to operate in a specific range of wave conditions and therefore the performance varies more abruptly with the location selected. Therefore, and given the results obtained in the present study, the selection of the most appropriate WEC-site combination proposed in this work requires an exhaustive cost analysis, which is out of the scope of this work.

All in all, the results show the importance of implementing specific procedures for wave resource analysis allowing the accurate computation of different intra-annual performance parameters leading to an informed decision-making when installing a wave farm in a region. At the present time WEDGE-p[®] tool is only available for the Galician coast; however, it could be developed and implemented to any other coastal region where long-term offshore wave data are available. In future work, the tool is expected to be extended throughout the Atlantic Region of Europe.

Acknowledgements

WEDGE-p[®] tool is the result of an extensive work developed in the framework of several research projects supported by the Ministry of Science and Innovation: *Evaluación de los Recursos Energéticos Renovables* (Ref. DPI2009-14546-CO2-02), Xunta de Galicia: *Consolidación e estruturación* – 2016 CIGEO (Ref ED431B 2019/30), Fundación Iberdrola: *Online Application and High Resolution Management System for the Exploitation of the Wave Energy Resource in the Atlantic Region of Europe*, and Fundación Barrié: *Development of a Geospatial Database for the*

Exploitation of the Wave Energy Resource along the Galician Coast. During this work I. López was supported by the postdoctoral grant ED481B 2016/125-0 of the ‘Programa de Axudas á etapa posdoutoral da Xunta de Galicia’. The authors are grateful to Puertos del Estado for providing the wave data, and to Instituto Español de Oceanografía (IEO) and Instituto Tecnológico para o Control do Medio Mariño de Galicia (Intecmar) for the ocean uses and environmental data.

List of symbols and abbreviations

WEC	wave energy converter
ICZM	integrated coastal zone management
WEDGE-p	Wave Energy Diagram Generator – performance
OTD	overtopping device
OWC	oscillating water column
WAB	wave activated body
GIS	geographic information system
P	power output
H_{m0}	spectral significant wave height
T_e	wave energy period
θ_m	mean wave direction
SWAN	Simulating Waves Nearshore
N	wave action density

437	t	time
438	C	propagation velocity in the geographical space
439	θ	direction of the waves
440	σ	relative frequency
441	C_θ	propagation velocity in the θ - space
442	C_σ	propagation velocity in the σ - space
443	S_t	source term
444	S_{in}	generation by wind source term
445	S_{nl3}	triad wave-wave interaction source term
446	S_{nl4}	quadruplet wave-wave interaction source term
447	S_{wc}	whitecapping source term
448	S_f	bottom friction source term
449	S_{br}	wave breaking source term
450	E_0	energy production
451	P_i	power output of a specific bin as provided by the power matrix
452	$O_{b,i}$	occurrence of a bin as provided by the characterization matrix
453	C_f	capacity factor
454	P_r	rated power
455	h	number of hours
456	CW	capture width

457 J available power

458 CWR capture width ratio

459 B characteristic dimension of the WEC

460

461 **References**

- 462 [1] Penalba M, Ulazia A, Ibarra-Berastegui G, Ringwood J, Sáenz J. Wave energy
 463 resource variation off the west coast of Ireland and its impact on realistic wave energy
 464 converters' power absorption. *Applied Energy* 2018;224:205-19.
- 465 [2] Fadaeenejad M, Shamsipour R, Rokni SD, Gomes C. New approaches in harnessing
 466 wave energy: With special attention to small islands. *Renewable and Sustainable*
 467 *Energy Reviews* 2014;29:345-54.
- 468 [3] Fernandez H, Iglesias G, Carballo R, Castro A, Fraguela JA, Taveira-Pinto F et al.
 469 The new wave energy converter WaveCat: Concept and laboratory tests. *Mar Struct*
 470 2012;29:58-70.
- 471 [4] Martins JC, Goulart MM, Gomes MdN, Souza JA, Rocha LAO, Isoldi LA et al.
 472 Geometric evaluation of the main operational principle of an overtopping wave energy
 473 converter by means of Constructal Design. *Renewable Energy* 2018;118:727-41.
- 474 [5] John Ashlin S, Sannasiraj SA, Sundar V. Performance of an array of oscillating
 475 water column devices integrated with an offshore detached breakwater. *Ocean*
 476 *Engineering* 2018;163:518-32.

- 477 [6] Medina-López E, Bergillos RJ, Moñino A, Clavero M, Ortega-Sánchez M. Effects
478 of seabed morphology on oscillating water column wave energy converters. *Energy*
479 2017;135:659-73.
- 480 [7] Rezanejad K, Guedes Soares C, López I, Carballo R. Experimental and numerical
481 investigation of the hydrodynamic performance of an oscillating water column wave
482 energy converter. *Renewable Energy* 2017;106:1-16.
- 483 [8] Zanuttigh B, Angelelli E, Kofoed JP. Effects of mooring systems on the
484 performance of a wave activated body energy converter. *Renewable Energy*
485 2013;57:422-31.
- 486 [9] Gunawardane SDGSP, Folley M, Kankanamge CJ. Analysis of the hydrodynamics
487 of four different oscillating wave surge converter concepts. *Renewable Energy*
488 2019;130:843-52.
- 489 [10] Carballo R, Iglesias G. A methodology to determine the power performance of
490 wave energy converters at a particular coastal location. *Energy Conversion and*
491 *Management* 2012;61:8-18.
- 492 [11] Carballo R, Sánchez M, Ramos V, Castro A. A tool for combined WEC-site
493 selection throughout a coastal region: Rias Baixas, NW Spain. *Applied Energy*
494 2014;135:11-9.
- 495 [12] Lenee-Bluhm P, Paasch R, Özkan-Haller HT. Characterizing the wave energy
496 resource of the US Pacific Northwest. *Renewable Energy* 2011;36:2106-19.

497 [13] Neill SP, Hashemi MR. Wave power variability over the northwest European shelf
498 seas. *Appl Energy* 2013;106:31-46.

499 [14] Carballo R, Sánchez M, Ramos V, Fraguera JA, Iglesias G. The intra-annual
500 variability in the performance of wave energy converters: A comparative study in N
501 Galicia (Spain). *Energy* 2015;82:138-46.

502 [15] Arean N. A comprehensive decision-making tool for wave energy exploitation: A
503 case study in the North coast of Galicia. 2016.

504 [16] Lange M, O'Hagan AM, Devoy RRN, Le Tissier M, Cummins V. Governance
505 barriers to sustainable energy transitions – Assessing Ireland's capacity towards marine
506 energy futures. *Energy Policy* 2018;113:623-32.

507 [17] Alexander K, Wilding T, Jacomina Heymans J. Attitudes of Scottish fishers
508 towards marine renewable energy. *Marine Policy* 2013;37:239-44.

509 [18] de Groot J, Campbell M, Ashley M, Rodwell L. Investigating the co-existence of
510 fisheries and offshore renewable energy in the UK: Identification of a mitigation agenda
511 for fishing effort displacement. *Ocean & Coastal Management* 2014;102:7-18.

512 [19] Castro-Santos L, Garcia GP, Simões T, Estanqueiro A. Planning of the installation
513 of offshore renewable energies: a GIS approach of the Portuguese roadmap. *Renewable*
514 *Energy* 2018.

515 [20] Babarit A. A database of capture width ratio of wave energy converters. *Renewable*
516 *Energy* 2015;80:610-28.

- 517 [21] Babarit A, Hals J, Muliawan MJ, Kurniawan A, Moan T, Krokstad J. Numerical
518 benchmarking study of a selection of wave energy converters. *Renewable Energy*
519 2012;41:44-63.
- 520 [22] A Weinstein, G Fredikson, MJ Parks, K Neislen. AquaBuOY - the offshore wave
521 energy converter: Numerical modeling and optimization. In *Proceedings of Ocean '04*
522 *MTS/IEEE Techno-Ocean '04* 2004;4:1854-9.
- 523 [23] Poullikkas A. Technology prospects of wave power systems. *Electronic Journal of*
524 *Energy & Environment* 2014.
- 525 [24] Project LifeDemoWave. Demonstration of the efficiency & environmental impact
526 of wave energy converters (WEC) in high energy coasts (LIFE14 CCM/ES/001209).
527 European Commission. ;2015-18.
- 528 [25] Carballo R, Arean N. WEDGE-p: Wave Energy Diagram Generator - performance.
529 2017;03/2017/1194.
- 530 [26] Silva D, Rusu E, Guedes Soares C. Evaluation of Various Technologies for Wave
531 Energy Conversion in the Portuguese Nearshore. *Energies* 2013:1344-64.
- 532 [27] Carballo R, Sánchez M, Ramos V, Taveira-Pinto F, Iglesias G. A high resolution
533 geospatial database for a wave energy exploitation. *Energy* 2014;68:572-83.
- 534 [28] Akpinar A, Kömürcü MI. Wave energy potential along the south-east coasts of the
535 Black Sea. *Energy* 2012;42:289.

- 536 [29] Kim G, Jeong WM, Lee KS, Jun K, Lee ME. Offshore and nearshore wave energy
537 assessment around the Korean Peninsula. *Energy* 2011;36:1460-9.
- 538 [30] Rusu E, Soares CG. Wave energy pattern around the Madeira Islands. *Energy*
539 2012;45:771-85.
- 540 [31] Silva D, Martinho P, Guedes Soares C. Wave energy distribution along the
541 Portuguese continental coast based on a thirty three years hindcast. *Renewable Energy*
542 2018;127:1064-75.
- 543 [32] Lavidas G, Venugopal V. Application of numerical wave models at European
544 coastlines: A review. *Renewable and Sustainable Energy Reviews* 2018;92:489-500.
- 545 [33] Iglesias G, Carballo R. Wave energy potential along the Death Coast (Spain).
546 *Energy* 2009;34:1963-75.
- 547 [34] Holthuijsen LH. *Waves in Oceanic and Coastal Waters*. Cambridge, U.K.:
548 Cambridge University Press, 2007.
- 549 [35] Carballo R. A holistic methodology cum database for wave energy exploitation:
550 Implementation on the Galician coast (NW, Spain). 2016.
- 551 [36] Bergillos RJ, López-Ruiz A, Medina-López E, Moñino A, Ortega-Sánchez M. The
552 role of wave energy converter farms on coastal protection in eroding deltas, Guadalfeo,
553 southern Spain. *Journal of Cleaner Production* 2018;171:356-67.

- [37] Rodriguez-Delgado C, Bergillos RJ, Ortega-Sánchez M, Iglesias G. Wave farm effects on the coast: The alongshore position. *Science of The Total Environment* 2018;640-641:1176-86.
- [38] Carballo R, Iglesias G. Wave farm impact based on realistic wave-WEC interaction. *Energy* 2013;51:216-29.
- [39] Rodriguez-Delgado C, Bergillos RJ, Ortega-Sánchez M, Iglesias G. Protection of gravel-dominated coasts through wave farms: Layout and shoreline evolution. *Science of The Total Environment* 2018;636:1541-52.

Figure captions

Figure 1. Spatial distribution of the marine uses and protected environmental zones within the coastal area of study (NW Spain) pinpointing the locations of the selected sites (Points A, B and C) of interest for installing a wave farm.

Figure 2. Power matrices a) Aquabuoy, b) Bref-HB and c) F2-HB, expressed in terms of power output (kW) for the different wave conditions (intervals of significant wave height, H_{m0} , and energy period, T_e).

Figure 3. Bathymetric configuration of the study area as interpolated into the numerical grid.

Figure 4. Omnidirectional annual wave resource characterization matrices at the offshore buoy location and at Points A, B and C (resolution 0.5 s x 0.5 m). [The numbers represent the occurrence expressed in hours in an average year; the isolines,

575 the wave power; and the colour scale, the total energy provided by each energy bin in an
576 average year.]

577 Figure 5. Wave resource characterization matrices of January and July at Points A, B
578 and C (resolution 1 s x 0.5 m)

579 Figure 6. Monthly energy production, E_o , (above) and capacity factor, C_f , (below) for
580 the different WECs considered at Point A.

581 Figure 7. Monthly energy production, E_o , (above) and capacity factor, C_f , (below) for
582 the different WECs considered at Point B.

583 Figure 8. Monthly energy production, E_o , (above) and capacity factor, C_f , (below) for
584 the different WECs considered at Point C.

585 Figure 9. Monthly capture width, CW , (above) and capture width ratio, CWR , (below)
586 for the different WECs considered at Point A.

587 Figure 10. Monthly capture width, CW , (above) and capture width ratio, CWR , (below)
588 for the different WECs considered at Point B.

589 Figure 11. Monthly capture width, CW , (above) and capture width ratio, CWR , (below)
590 for the different WECs considered at Point C.

Table 1

Table 1. Characteristics of WECs selected

WEC	Complete WEC designation	P_r (kW)	Recommended depth (m)
Aquabuooy	Aquabuooy	250	50-100
Bref-HB	Small bottom-referenced heaving buoy	15	40-100
F-2HB	Floating two-body heaving converter	1000	50-100

Table 2

Table 2. Type and characteristic dimension, B [m], of WECs selected

WEC	Type of WEC	Dimension	B [m]	Ref.
Aquabuooy	Floating heaving device	Diameter of floating body	6	[22]
Bref-HB	Bottom-fixed heaving device	Diameter of floating body	3	[21]
F-2HB	Floating heaving device	Diameter of floating body	20	[21]

Figure 1

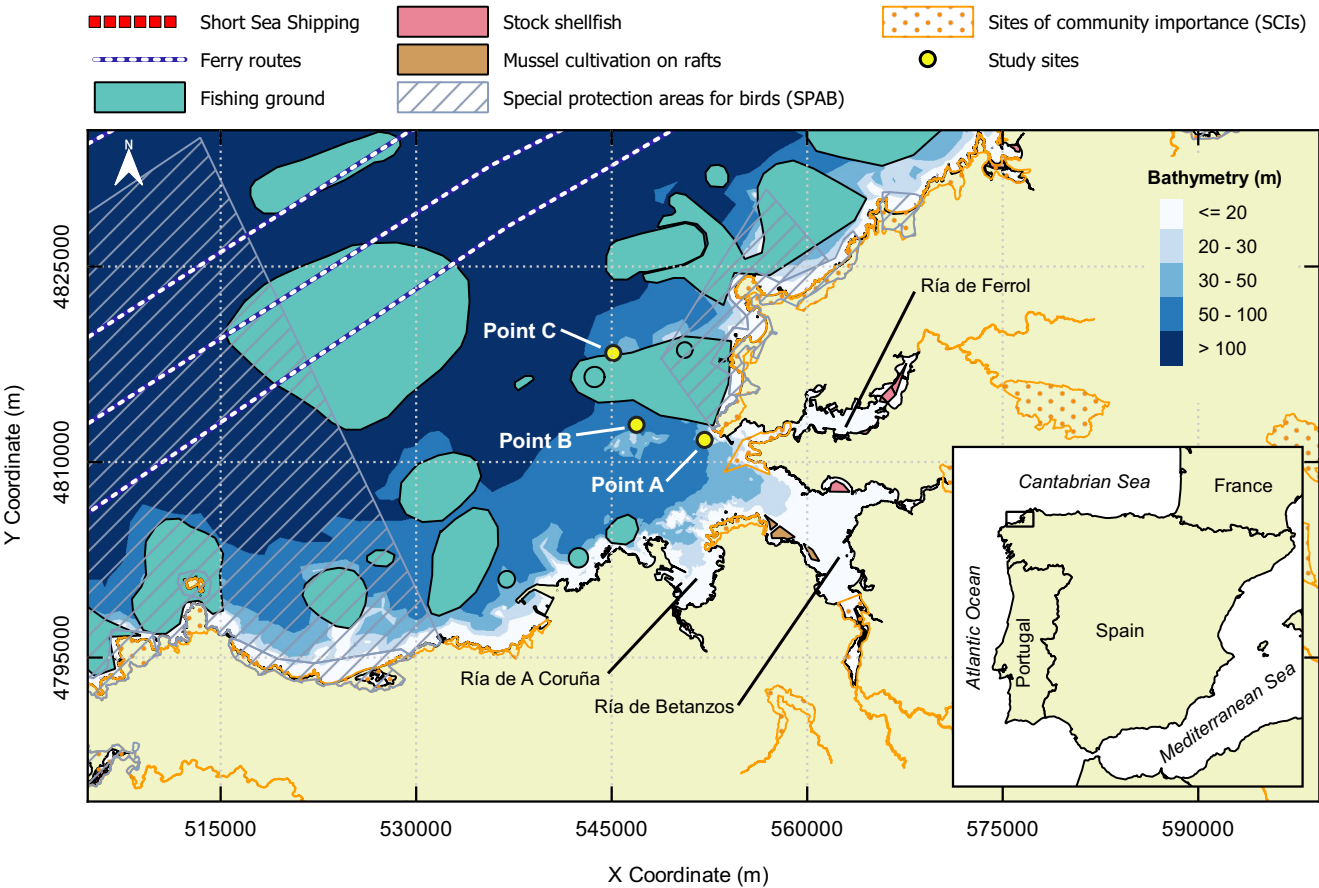


Figure 2

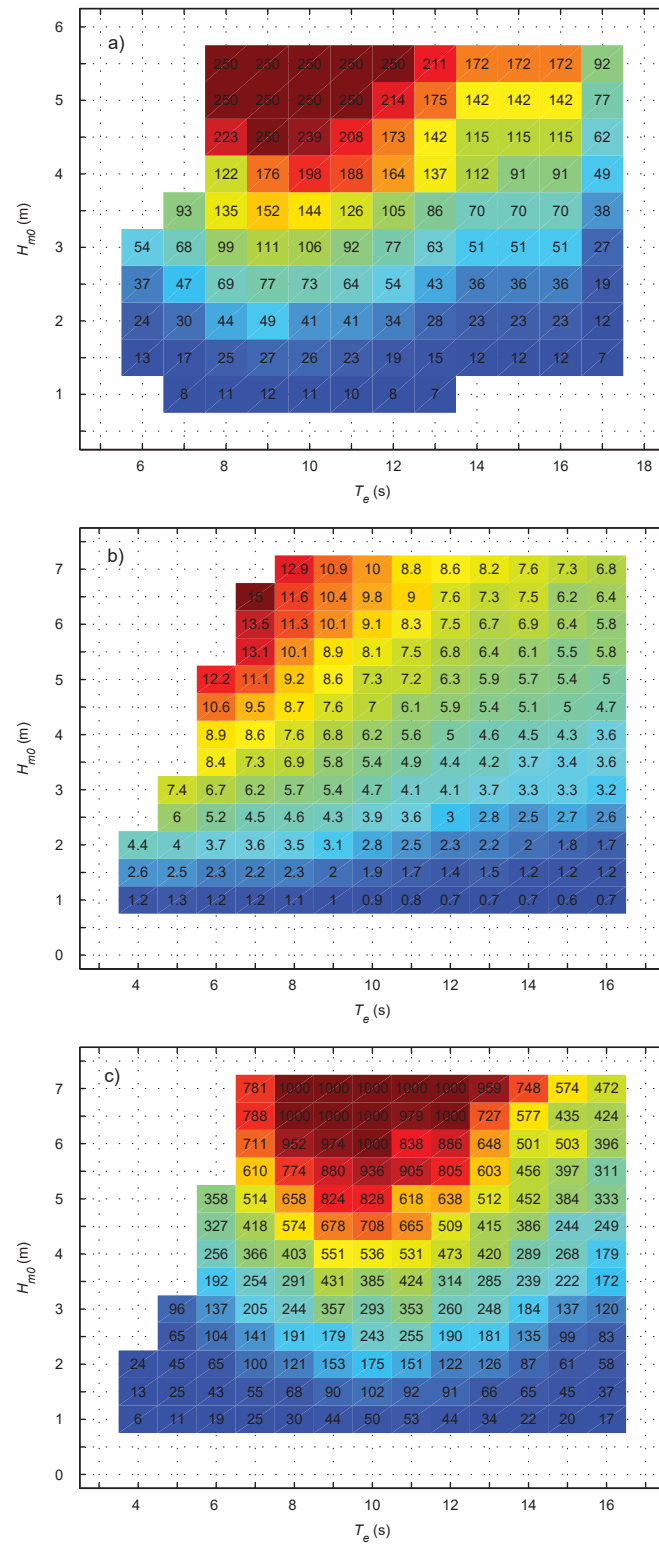


Figure 3

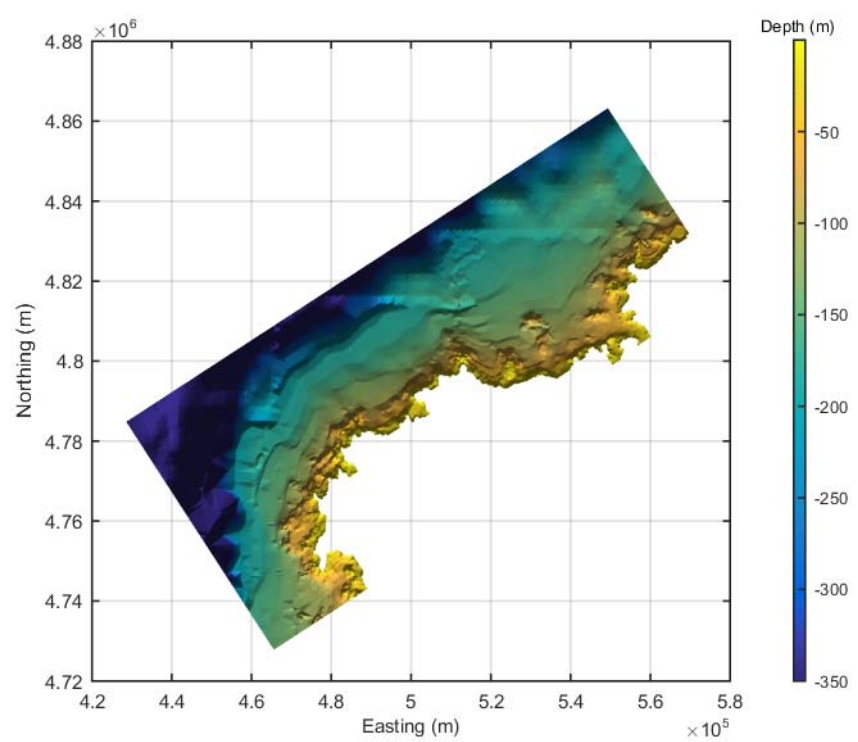


Figure 4

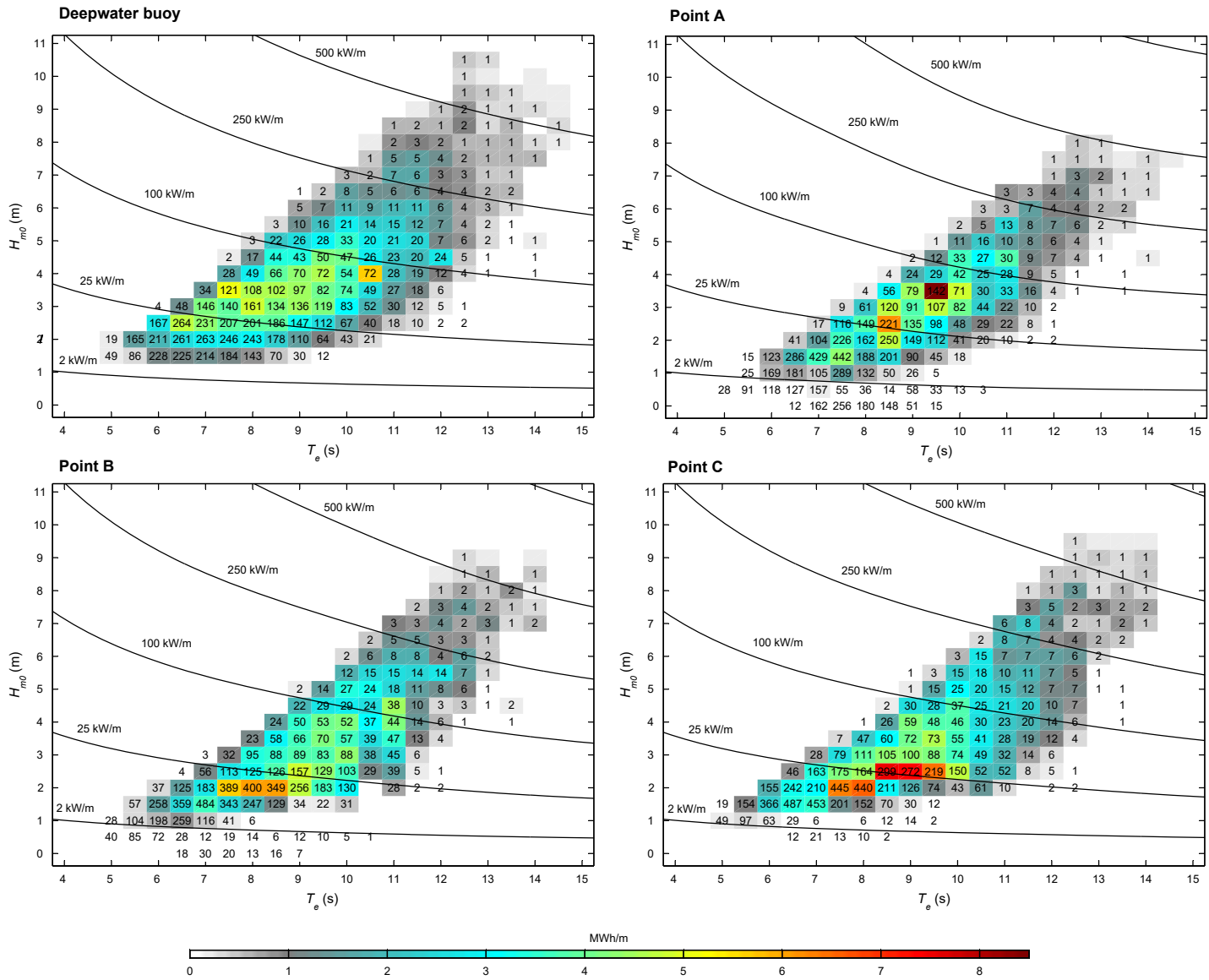


Figure 5

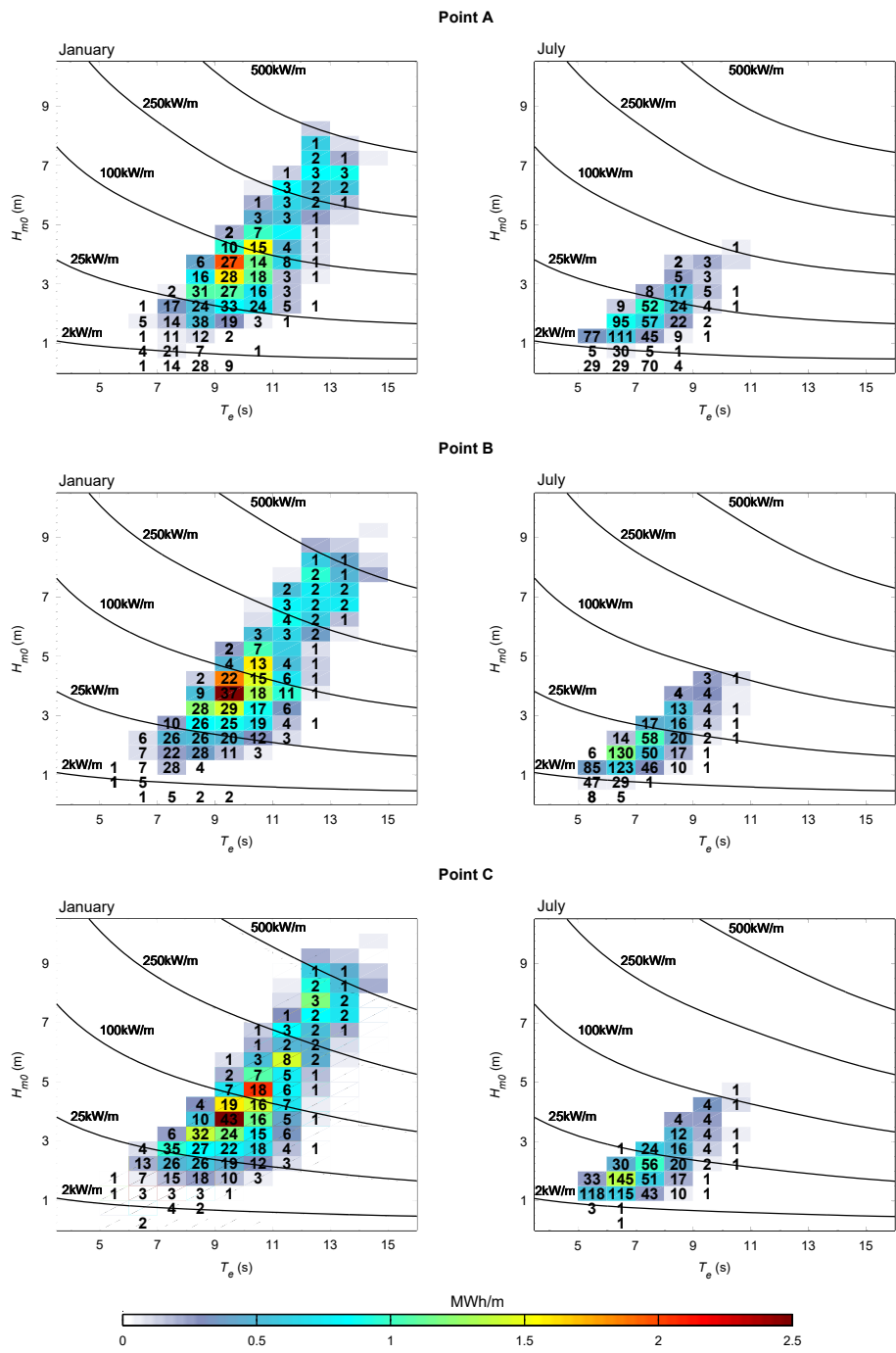


Figure 6

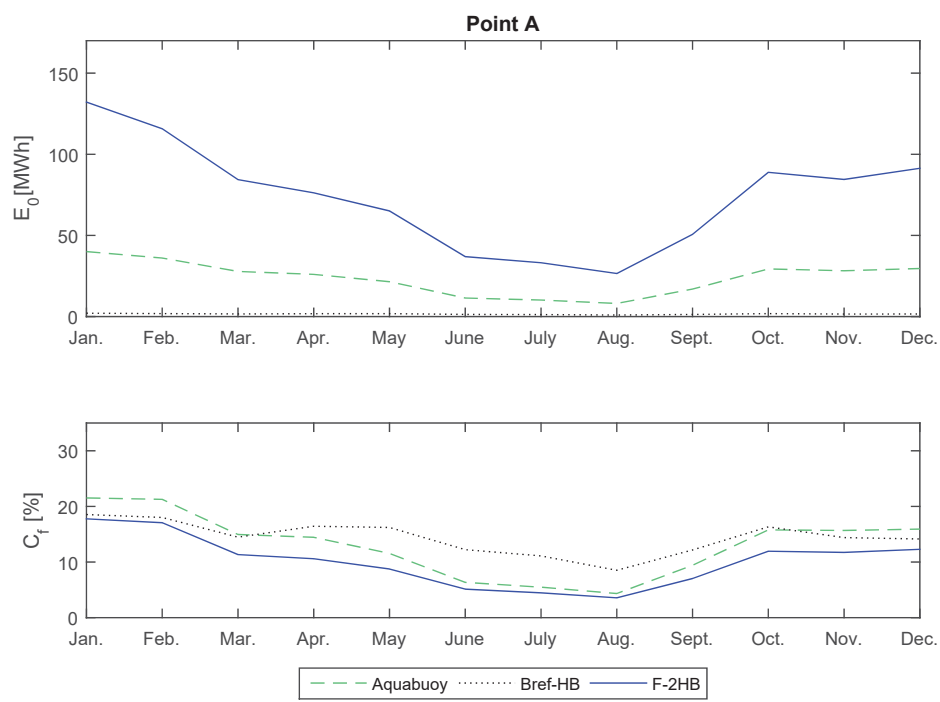


Figure 7

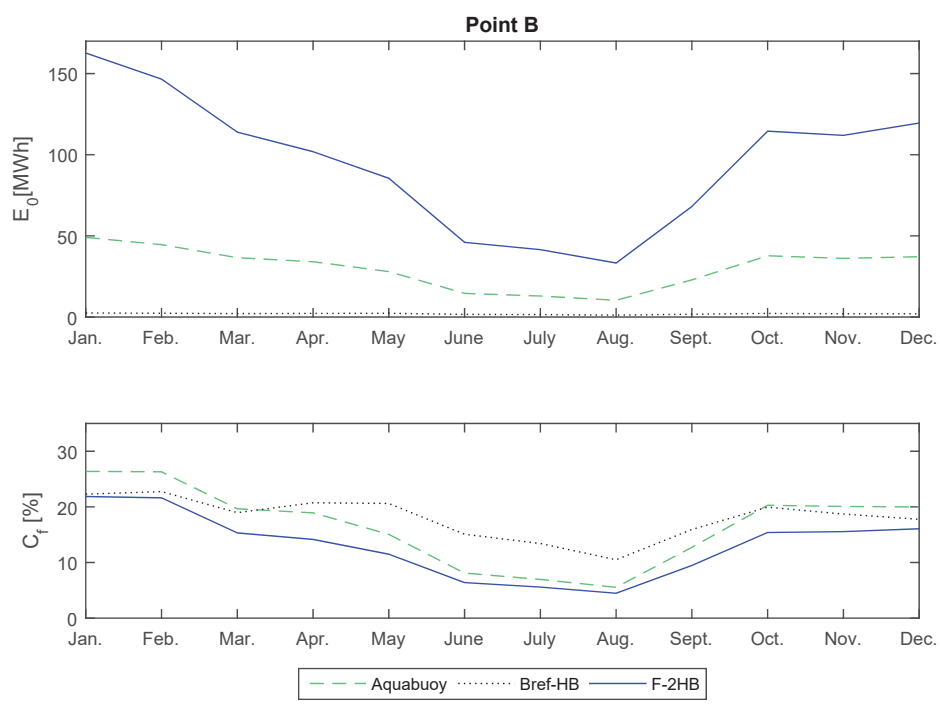


Figure 8

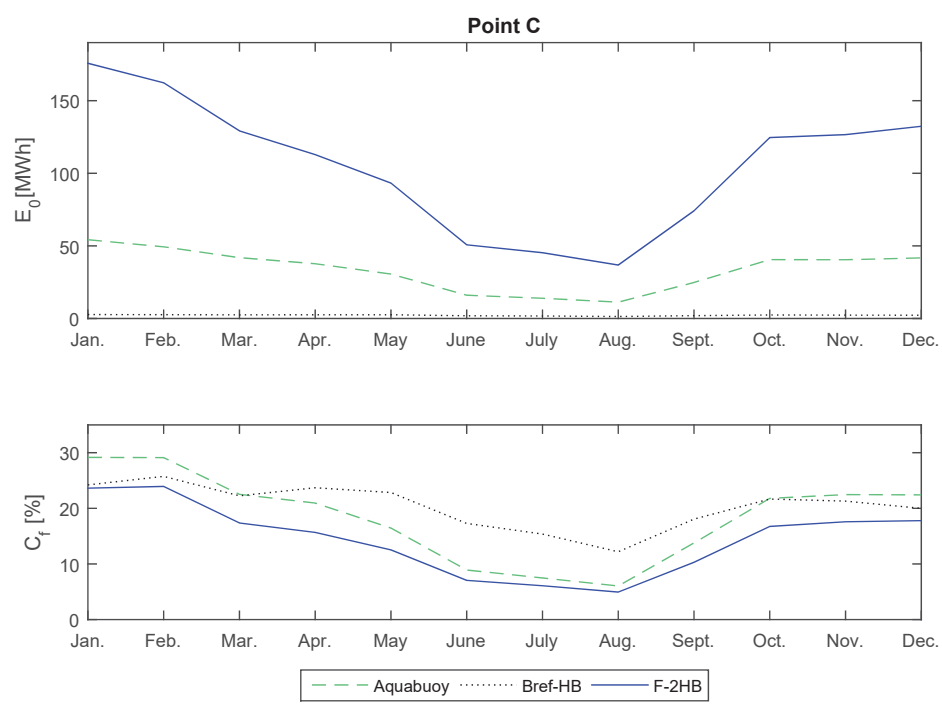


Figure 9

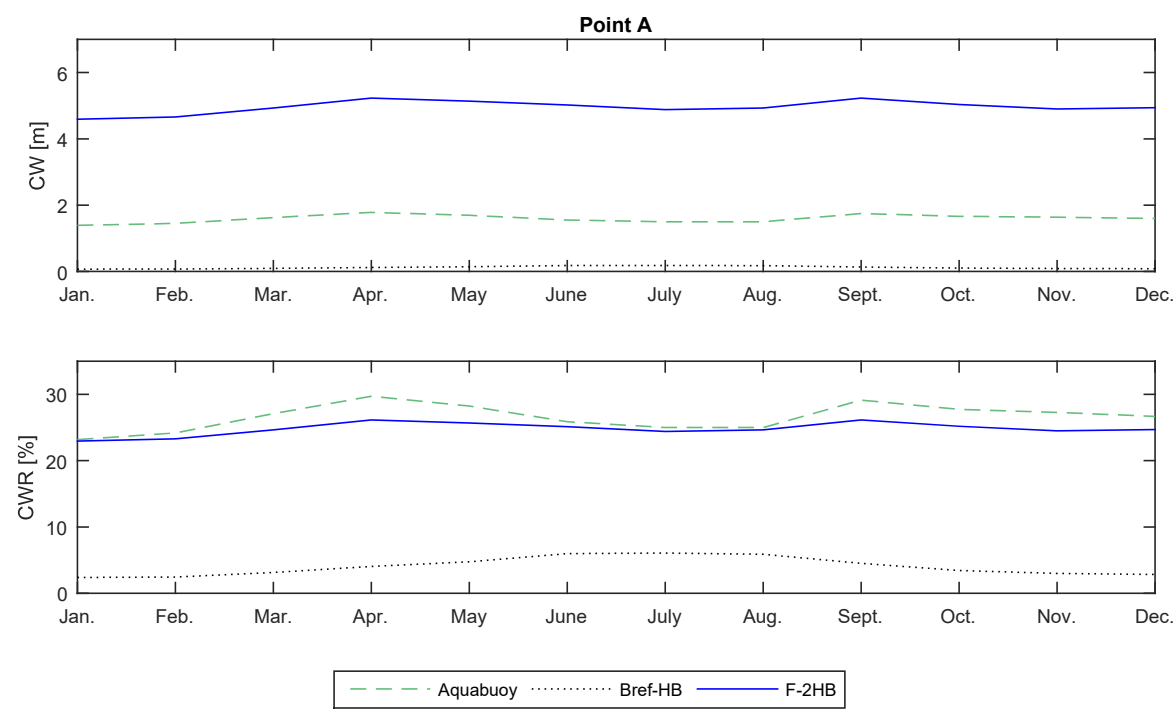


Figure 10

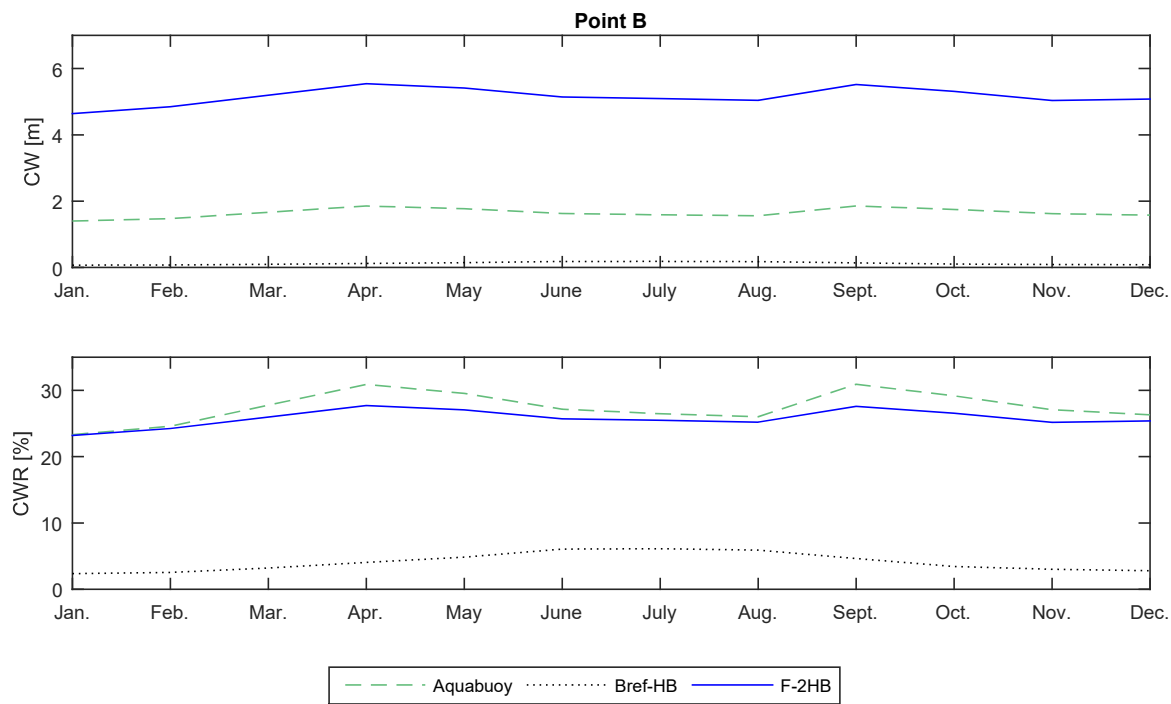


Figure 11

